JOURNAL OF Materials CHEMISTRY

High pressure synthesis and crystal structure of a new Ni(III) perovskite: $TlNiO_3$

Seung-Joo Kim,[a] Gérard Demazeau,*[a] José A. Alonso[b] and Jin-Ho Choy[c]

[a]*Institut de Chimie de la Matière Condensée de Bordeaux (ICMCB), UPR-CNRS 9048, 87 Avenue de Dr. A. Schweitzer, 33608 Pessac cedex, France. E-mail: demazeau@icmcb.u-bordeaux.fr*
[b]*Instituto de Ciencia de Materiales de Madrid (CSIC) Cantoblanco, E-28045 Madrid, Spain*
[c]*National Nanohybrid Materials Laboratory, School of Chemistry and Molecular Engineering, Seoul National University, Seoul 151-747, Korea*

Received 30th August 2000, Accepted 15th November 2000
First published as an Advance Article on the web 4th January 2001

A new Ni(III) compound, $TlNiO_3$ has been prepared under high oxygen pressure. The pressure and temperature domain required to prepare pure $TlNiO_3$ was found to be very narrow ($P \geqslant 7.5$ GPa, $650 \leqslant T \leqslant 700$ °C). $TlNiO_3$ crystallizes in the $GdFeO_3$-type perovskite structure with the following lattice parameters: $a = 5.2549(1)$, $b = 5.3677(1)$ and $c = 7.5620(2)$ Å. The corresponding unit cell volume of 213.3 Å^3 is somewhat larger than the value expected from a plot of unit cell volume *vs.* ionic radius of the A cation for the analogous $ANiO_3$ series (A = rare earth metal or yttrium). According to the structural analysis, the twelve Tl–O bonds in $TlNiO_3$ can be classified into three approximate groups (four short, four medium and four long distances), while, in the other $ANiO_3$ compounds, the A–O bonds are divided into two groups of eight short and four long distances. The large unit cell volume of $TlNiO_3$ is surely due to the different coordination of the Tl(III) ion in the perovskite lattice. The average Ni–O–Ni bond angle (147.6°) in $TlNiO_3$ is very similar to that observed in $YNiO_3$ (147.3°). However, the Néel temperature ($T_N = 105$ K) in antiferromagnetic $TlNiO_3$ is significantly lower than that observed in $YNiO_3$ ($T_N = 145$ K), which has a comparable Ni–O–Ni angle. The magnetic properties could be explained by the competing effect of the Tl(III)–O bond on the covalency of Ni(III)–O bond.

Introduction

Since the first synthesis of the $ANiO_3$ (A = rare earth or yttrium) perovskites series,[1] much research has been devoted to understanding their physical properties. The $ANiO_3$ family undergoes a transition from Pauli paramagnetism in metallic $LaNiO_3$ to Curie–Weiss paramagnetism with antiferromagnetic ordering below T_N in $YNiO_3$ and $LuNiO_3$.[2,3] Recently, the transition from low temperature insulating state to high temperature metallic state was discovered in all the $ANiO_3$ family, except for $LaNiO_3$, and it was also found that the transition temperature (T_{MI}) increases systematically with decreasing size of the rare earth ions.[4–10] The continuous and monotonic dependence of T_N and T_{MI} upon structural distortion for these oxides provides a great opportunity to verify several empirical and theoretical results concerning magnetism and metal–insulator transitions.[5,7,9,10]

Structural distortion in ABO_3 perovskites due to a mismatch between the A–O and B–O bond distances has been discussed in terms of the geometrical tolerance factor, t:

$$t = d_{A-O}/2^{1/2}d_{B-O}$$

The bond distances are calculated from the sum of ionic radii. In the ideal perovskite structure ($t = 1$), the A cation is surrounded by twelve oxygen ions in a regular dodecahedral environment. If the A cation is replaced by a smaller ion ($t < 1$), the BO_6 octahedra would rotate cooperatively about the cubic crystallographic axis, giving rise to a tilted B–O–B bond angle with a reduction in the coordination number of the A cation, in order to relieve the structural stress. The A cation coordination number is determined by the number of oxygen ions that can be fitted around the cation. The simple ionic lattice model, based on the treatment of ions as hard spheres with point charges, is fairly useful in describing ionic compounds.

However, covalent bonding interactions must also be considered in order to understand details of the relationship between structural distortion and physical properties, because the bonding in perovskites is well known to be intermediate between the extremes of ionic and covalent bonding.[11] Concerning Ni(III) perovskites, most comparative studies have been carried out on compounds containing rare earth ions or yttrium. In these cases, it is hard to investigate the electronic effect of the A cation on structural distortion and physical properties because all rare earth and yttrium ions bond to oxygen with similar covalency. From this viewpoint, a post transition metal ion, *e.g.* Tl(III), is a good candidate for the A cation in ABO_3 perovskites because it has fully occupied 4f and 5d orbitals ([Xe] $4f^{14}$ $5d^{10}$ $6s^0$) in contrast to trivalent rare earth ions ([Xe] $4f^n$ $5d^0$ $6s^0$, $0 \leqslant n \leqslant 14$). Two Tl(III) compounds, $TlFeO_3$ and $TlCrO_3$, have already been prepared some thirty years ago,[12] but no further study has been made, probably due to the difficulty of preparation.

The present work is focussed on the synthesis and the structural characterization of a new perovskite, $TlNiO_3$. The high oxygen pressure technique would be required for the stabilization of Ni(III) in perovskite lattice.[1,2] Under high pressure, moreover, anions are more easily compressed compared to cations, which leads to an increase in the coordination numbers of cations and, therefore, enhances the stability of perovskite structures with smaller A cations, such as Tl(III). A comparative analysis of the structural distortion and magnetic properties of $TlNiO_3$ compared to analogous $ANiO_3$ (A = rare earth ion or yttrium) materials is also presented.

DOI: 10.1039/b007043m

Experimental

The perovskite, $TlNiO_3$, was prepared under high pressure–high temperature (HP–HT) conditions with a "Belt"-type apparatus. Tl_2O_3 and $Ni(OH)_2$ were used as starting materials. The nickel content in the $Ni(OH)_2$ was carefully determined by thermogravimetry before use. Stoichiometric amounts of these materials were mixed with an oxidizing agent, $KClO_3$, in the molar ratio $Tl_2O_3 : Ni(OH)_2 : KClO_3 = 1 : 2 : 1$. The reactants, encapsulated in a gold tube with a diameter of 3 mm, were placed in the center of a graphite tube (internal heater) with an inner diameter of 5 mm. Sodium chloride powder filled the space between the heater and the gold capsule, forming an electrically insulating barrier and improving pressure homogeneity. The temperature was checked during the experiment by means of a thermocouple placed near the gold capsule. Successful synthesis was achieved under the HP–HT conditions 7.5–9 GPa and 650–700 °C for 2–3 min. The reaction expected to occur during the HP–HT procedure is as follows:

$$Tl_2O_3 + 2Ni(OH)_2 + KClO_3 \rightarrow 2TlNiO_3 + KCl + 2H_2O + O_2\uparrow$$

After the HP–HT reaction, the product was quenched, washed with distilled water to remove the potassium chloride, and then dried at 120 °C.

The total oxygen content of the sample was determined by iodometric titration under an inert atmosphere (N_2). The reduction of $TlNiO_{3-\delta}$ by iodide in aqueous solution may be written as:

$$TlNiO_{3-\delta}(s) + (3-2\delta)I^-(aq) + 2(3-\delta)H^+(aq) \rightarrow$$
$$TlI(s) + Ni^{2+}(aq) + (3-2\delta)/2I_2(aq) + (3-\delta)H_2O$$

The liberated iodine was determined by titration with a standard sodium thiosulfate solution. Typically, 15 mg of $TlNiO_{3-\delta}$ was dissolved in 6 M HCl solution (*ca.* 10 ml) containing an excess of potassium iodide. Carbon tetrachloride (*ca.* 15 ml) was used as the indicator to prevent interference due to the yellowish color of the Tl(I) precipitate. After vigorous shaking of the organic–aqueous bi-phasic solution, the greater part of the iodine in the aqueous layer is transferred to the organic layer due to the high solubility of iodine in carbon tetrachloride. The end point was marked by the disappearance of the pink color in the carbon tetrachloride solution.[13]

The thermal behavior of $TlNiO_3$ was monitored by thermogravimetry (TG) with a MTB10-8 STRAM balance under an oxygen atmosphere ($P_{O_2} = 1$ bar). The sample was heated at a rate of 5 °C min^{-1} from 20 to 650 °C.

Powder X-ray diffraction profiles were recorded on a Philips PW 1050 diffractometer using graphite-monochromated Cu-Kα radiation. Data were collected over the 2θ range 10–110° for 10 s in each 0.02° step at ambient temperature. The structural parameters were refined with the Rietveld program FULLPROF.[14] The background level was optimized with a polynomial function and the peak shape was fitted to a pseudo-Voïgt function.

DC magnetic susceptibility was measured using a SQUID magnetometer (Quantum Design MPMS) in the temperature range 5–300 K at 10 000 G after zero-field cooling.

Results and discussion

Synthesis

Efforts were made to optimize the synthetic conditions by changing various reaction parameters *i.e.* temperature, pressure, time and precursors. The preparation of $TlNiO_3$ was at first attempted using Tl_2O_3 and NiO as reactants. The perovskite phase, $TlNiO_3$, was partially produced in the narrow temperature range 650–700 °C at high pressure (beyond 7.5 GPa). However, a small amount of aggregated thallium(III) oxide and nickel oxide still remained, together with the main perovskite phase. This phenomenon has been attributed to the temperature/pressure gradient in the "Belt"-type high pressure apparatus; it appeared in all cases where nickel oxide was used within a reaction time of 15–60 min. In this case, the phase formation was strongly dependent on particle size when nickel oxide was used: the smaller the particles are, the better the result from the HP–HT reaction. When the reaction mixture was heated at temperatures above 800 °C under a pressure of 7.5 GPa, the resulting products were thallium(III) oxide (high pressure phase), nickel oxide and potassium chloride, with no trace of the perovskite phase being found. This implies that $TlNiO_3$, once formed, might be re-decomposed to the corresponding oxides under such conditions. It was, therefore, crucial to search for a precursor with a reactivity high enough to transform completely to the perovskite phase at a relatively low temperature. The pure perovskite phase was obtained only after replacing nickel oxide with nickel hydroxide, $Ni(OH)_2$, as a starting material. A reaction time of 2–3 min was enough to produce monophasic $TlNiO_3$. $Ni(OH)_2$ significantly improved the reactivity and overcame the phase segregation problem due to the pressure gradient in this high pressure synthesis.

Total oxygen content and thermal stability for $TlNiO_3$

The total oxygen amount, $3-\delta$, in $TlNiO_{3-\delta}$ was determined to be 2.96 ± 0.02 after chemical titration, which is consistent with the TG result, as shown in Fig. 1. In the TG curve under an oxygen atmosphere, four main weight loss domains are observed for the temperature ranges 270–350, 390–430, 430–530, and >530 °C.

The first (270–350 °C) and second (390–430 °C) weight changes are attributed to released oxygen due to the reduction of Ni(III) to Ni(II). Assuming that the perovskite phase completely decomposes through the reaction $TlNiO_{3-\delta} \rightarrow Tl_2O_3 + NiO + \frac{1}{2}(1-\delta)O_2$ in these temperature ranges, the value of δ can estimated to be 0.01 from the difference between the observed weight loss (2.51%) and the theoretical value (2.57%) for the stoichiometric composition, $TlNiO_3$. The plateau in the TG curve around 370 °C presumably indicates the existence of an intermediate phase with a mixed Ni(II)/Ni(III) valence before further decomposition. Thus, the overall decomposition process in TG analysis can be expressed as follows:

$$TlNiO_{2.99} \xrightarrow[270-350\,^\circ C]{0.05\ O_2\uparrow} TlNiO_{2.89} \xrightarrow[390-430\,^\circ C]{0.195\ O_2\uparrow} \tfrac{1}{2}Tl_2O_3 + NiO$$

The third and fourth weight losses, which occur above 430 °C,

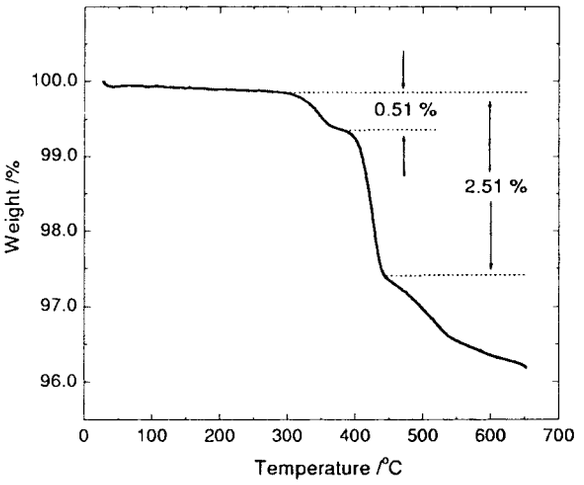

Fig. 1 Thermogravimetric analysis for $TlNiO_3$ under an oxygen atmosphere.

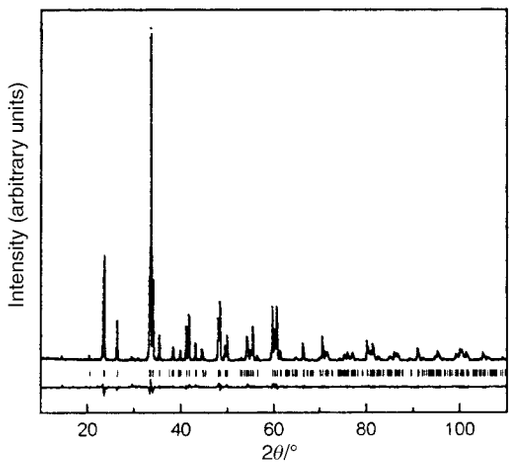

Fig. 2 Rietveld refinement profile for $TlNiO_3$ at room temperature. The filled circles (●) represent the experimental data, and the solid line is the calculated profile. The difference is plotted at the bottom of the figure. The upper set of tick marks indicates the Bragg positions of $TlNiO_3$.

may result from partial oxygen loss and subsequent sublimation of thallium sesquioxide, respectively.

Structure

All reflections in the powder XRD pattern of $TlNiO_3$ were indexed using a primitive orthorhombic unit cell. No systematic absences were found for the (*hkl*) or (*hk*0) reflections. For (*h*0*l*) and (0*kl*), only reflections with $h+l=$E (even) and $k=$E were observed, respectively. For the (*h*00), (0*k*0), and (00*l*) reflections, all *h*, *k*, and *l* were always found to be even. These systematic absences implythat $TlNiO_3$ either crystallizes in the space group *Pbnm* (standard group: *Pnam*) or $Pbn2_1$ (standard group: $Pna2_1$).[15] The diffraction data were refined with the space group *Pbnm*, assuming centrosymmetry for the nickel ions in the lattice.

The observed, calculated and difference patterns from Rietveld refinement are shown in Fig. 2. The structural parameters (lattice parameters, refined atomic positions, and isotropic temperature factors for all atoms), reliability factors, selected interatomic distances and angles are listed in Table 1.

The simulated structure of $TlNiO_3$ is represented in Fig. 3. The oxygen polyhedron around the Tl ion appears to be severely distorted. The Tl–O bond distances are spread over the range 2.235 to 3.381 Å. As a first approach, the twelve Tl–O bond distances can be divided into three groups: (i) four short bonds of 2.235–2.257 Å, (ii) four medium length bonds of 2.523–2.662 Å, and (iii) four long bonds of 3.097–3.380 Å.

The average Ni–O bond distance in $TlNiO_3$ is estimated as 1.960 Å, which is in good agreement with those in other nickelates. According to previous reports, the Ni–O bond distance of $ANiO_3$ increases gradually as the size of the A ion decreases, *i.e.* from 1.934 Å for $LaNiO_3$ to 1.961 Å for $DyNiO_3$, due to the diminished degree of electronic localization on the Ni–O bonds in the strongly distorted structure.[4,8,10]

In spite of the expected Jahn–Teller electronic configuration ($t_{2g}^6\ e_g^1$) for low spin Ni(III) in a localized system, it is known that NiO_6 octahedra are very regular in the perovskite structures with the space group *Pbnm*. It has been observed that the subtle anisotropic distortion increases slightly on going from $NdNiO_3$ to $DyNiO_3$. The distortion parameter (Δ_d), defined in Table 1, for NiO_6 octahedra in $TlNiO_3$ is 2.6×10^{-4}, which is somewhat large compared to other Ni(III) perovskites. (Δ_d values of 0.46, 0.32, 1.02, and 1.08×10^{-4} have been reported for Sm, Eu, Gd, and $DyNiO_3$, respectively.[8]) The average Ni–O–Ni angle in $TlNiO_3$ is 147.6° which is close to that of $DyNiO_3$.

Very recently, symmetry reduction from orthorhombic to monoclinic for $ANiO_3$ (A = Ho, Y, Er, Tm, Yb, Lu) due to the partial charge disproportionation of Ni^{3+} to $Ni^{3+\delta}$ and $Ni^{3-\delta}$ was observed from neutron diffraction experiments.[8–10] Such an effect cannot be ruled out for $TlNiO_3$ because of its structural similarity to these compounds, although such an effect is not detected in the powder XRD pattern. Further investigations on the electronic structure of nickel in $TlNiO_3$ are currently in progress.

Unit cell volume and local environment of Tl(III)

For $ANiO_3$ (A = rare earth or yttrium), the unit cell volume changes monotonically with respect to the ionic radius of the A cation, as reported previously.[1,8,10] When the unit cell volume of $TlNiO_3$ (213.3 $Å^3$) is compared to the plot of unit cell volume *vs.* ionic radius (*V vs. r* plot) for $ANiO_3$, the value obtained is close to that of $DyNiO_3$ (213.4 $Å^3$), and hence the ionic radius of Tl(III) can be estimated as *ca.* 1.02 Å, as shown in Fig. 4. However, the ionic radius of Tl(III) (0.98 Å for CN = 8) from Shannon[16] is somewhat different, but between the values for Lu(III) and Yb(III). It should be noted that such deviations are also observed for $TlFeO_3$ and $TlCrO_3$: their unit cell volumes are similar to those of $DyFeO_3$ and $DyCrO_3$, respectively.[12]

Table 1 Structural parameters,[a] main bond distances and selected bond angles for $TlNiO_3$

	Site	*G*	*x*	*y*	*z*	*B*/Å^2
Tl	4c	1	0.9860(2)	0.0486(1)	0.25	0.52(2)
Ni	4b	1	0.5	0	0	0.64(5)
O1	4c	1	0.095(2)	0.454(2)	0.25	0.5(3)
O2	8d	1	0.696(1)	0.297(2)	0.051(1)	0.7(2)

	Multiplicity	Bond distance/Å		Bond angle/°
Tl–O1	1	2.257(9)	O1–Ni–O2	87.1(5)
Tl–O1	1	2.253(10)	O1–Ni–O2	87.4(5)
Tl–O1	1	3.241(10)	O2–Ni–O2	89.1(6)
Tl–O1	1	3.097(9)		
Tl–O2	2	2.235(8)		
Tl–O2	2	2.523(8)	Ni–O1–Ni	147.1(1)
Tl–O2	2	2.662(7)	Ni–O2–Ni	147.8(3)
Tl–O2	2	3.381(8)	Δ_d[b]	2.6×10^{-4}
Ni–O1	2	1.971(3)		
Ni–O2	2	1.937(8)		
Ni–O2	2	1.972(8)		

[a] $R_{wp}=8.54$, $R_{exp}=5.44$, $R_{Bragg}=2.57\%$, $\chi^2=2.47$, $a=5.2549(1)$, $b=5.3677(1)$, $c=7.5620(2)$ Å, $Z=4$. [b] The distortion parameter, Δ_d, of an octahedron NiO_6 with an average Ni–O distance is defined as $\Delta_d=(1/6)\Sigma_{n=1,6}\{(d_n-\langle d\rangle)/\langle d\rangle\}^2$.

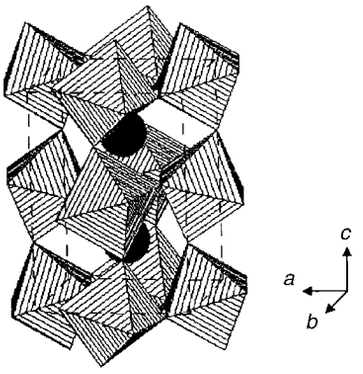

Fig. 3 Crystal structure model of $TlNiO_3$.

In order to understand such an anomalous structural aspect in $TlNiO_3$, we made an attempt to compare the A–O bond distances in several perovskites containing Ni(III). In an ideal cubic perovskite structure, the A cation is coordinated by twelve equidistant oxygen ions. If the A cation is substituted by a smaller ion, the AO_{12} dodecahedron becomes distorted, leading to a change in the distribution of A–O bond distances. It is well known that eight A–O bonds among the twelve become shorter and the other four gradually become longer as the size of the A cation decreases in the $GdFeO_3$-type structure.[17] This trend is clearly observed for the compounds containing small rare earth ions, as shown in Fig. 5, in which the A cation is coordinated to eight oxygen ions as the first-nearest neighbors and four other oxygen ions as second-nearest for the compounds from $PrNiO_3$ to $LuNiO_3$. The coordination number of the A cation can, therefore, be expressed as $8+4$ for these compounds. For $TlNiO_3$, however, the distribution of Tl–O bond distances shows an additional splitting of the eight short bonds into two groups of four short and four medium distances. And, as a consequence, the coordination number of thallium to oxygen can be approximated as $4+4+4$.

According to Alfred and Rochow's estimation,[19] the electronegativities are 1.44 for Tl and 3.40 for O, respectively, whereas the values for all the rare earth elements fall into the range 1.02–1.11. The Tl–O bonds are expected to be relatively covalent due to the small difference in electronegativity between them. The covalent bond interactions are dependent upon the spatial orbital overlap as well as the bond distances. The directional preference of the strong covalent character of the Tl(III)–O bond may lead to the uniquely distorted Tl–O polyhedron.

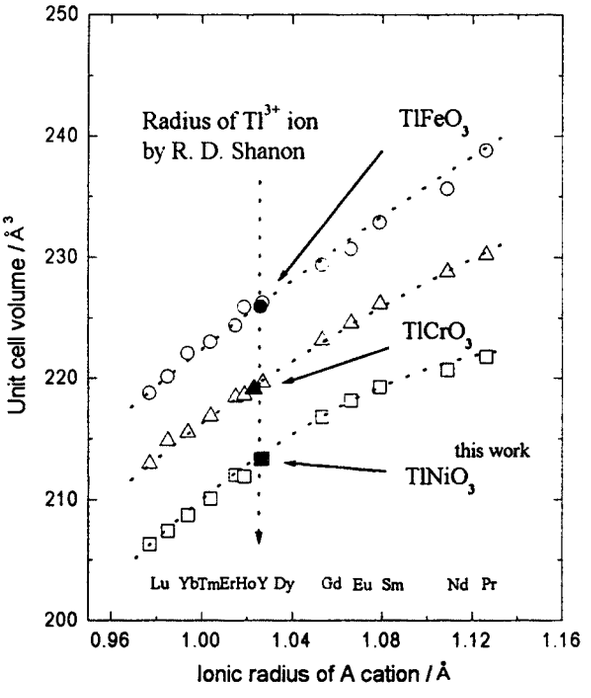

Fig. 4 Relation between ionic radii and unit cell volumes for $TlNiO_3$ and $ANiO_3$ [1] (A = rare earth or yttrium). The relations for $TlFeO_3$ [12]–$AFeO_3$ [17] and $TlCrO_3$ [12]–$ACrO_3$ [18] are also plotted for comparison.

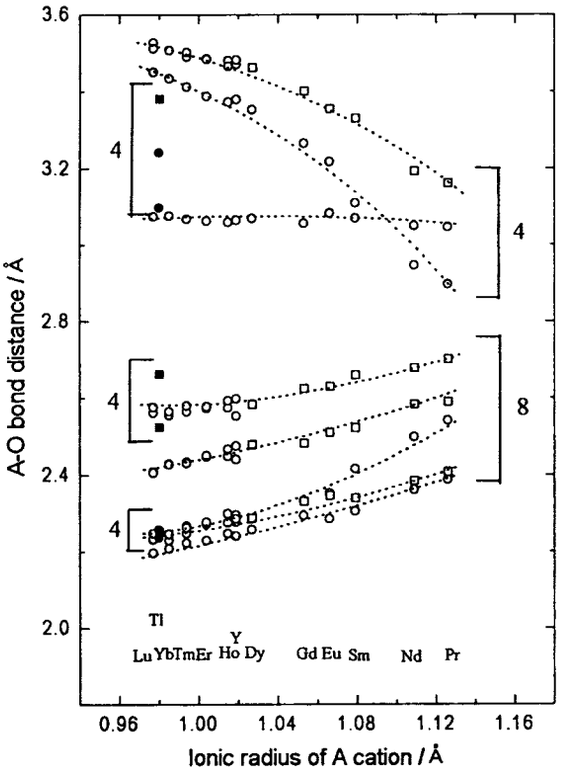

Fig. 5 Variation of the A–O bond distances on the ionic radius of the A cation in $ANiO_3$ (A = rare earth or yttrium). ○, □, ● and ■ represent the A–O1, A–O2, Tl–O1 and Tl–O2 bond distances, respectively. The multiplicities of A(Tl)–O1 and A(Tl)–O2 are 1 and 2, respectively. The bond distances for $ANiO_3$ (A = rare earth or yttrium) are plotted on the basis of values in ref. 5, 8 and 10.

One of useful method for describing the bonding nature in the present compound is Brown's bond valence model.[20] In this model, the ionic bond valence sum (BVS) should be constant from one structure to the next if the average bonding capacity of each ion remains unchanged between structures. As shown in Table 2, the bond valence sums for Ni and Tl show slightly negative and positive deviations, respectively. It should be noted that Tl exhibits a different aspect in comparison with rare earths or yttrium in the corresponding perovskites. For example, the bond valence for Dy within $\langle DyO_{12} \rangle$ polyhedra in $DyNiO_3$ is calculated to be 3.26 from the previously reported data.[8] This larger than expected bond valence (expected value 3.00) means that the average Dy–O distance in $DyNiO_3$ is somewhat shorter than the average bond distance observed in

Table 2 Coordination numbers (N), valences sum (V) and deviation from the expected charge [$\Delta V(\%) = 100(V-Q)/Q$] in $TlNiO_3$

	Tl	Ni	O1	O2
N	12	6	6	6
V^a	3.04	2.86	2.03	1.94
$\Delta V(\%)$	1.3	−4.7	1.5	−3.0

[a] V is the sum of individual bond valences (s_i) for Tl–O and Ni–O bonds. Bond valence are calculated as $s_i = \exp[(r_0 - r_i)/B]$; $B = 0.37$, $r_0 = 2.003$ for Ti(III)–O pairs, $r_0 = 1.686$ for Ni(III)–O pairs from ref. 20. Individual Tl–O and Ni–O distances (r_i) are taken from Table 1.

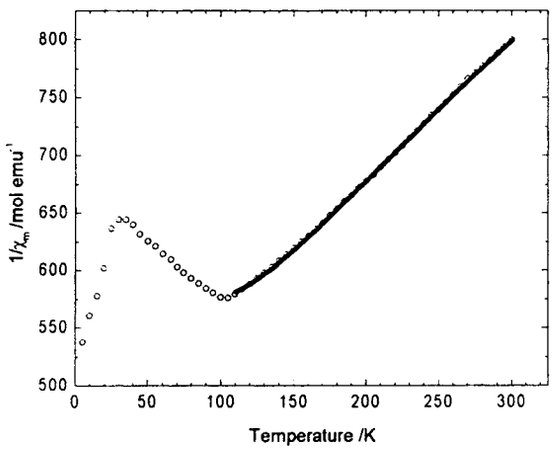

Fig. 6 Temperature dependence of the inverse molar magnetic susceptibility for $TlNiO_3$. The calculated values are presented as a solid curve.

other oxides containing Dy. This fact seems to indicate that the Dy cation is under compressive stress. The compressive stress on the Dy–O bond in $DyNiO_3$ could be released by keeping constant the bond distance but decreasing orbital overlap between Dy and O. It can also be expressed in a decreasing effective coordination number for Dy. However, the discrepancy between the observed bond valence and that expected for Tl(III) in $TlNiO_3$ is remarkably small, implying that there is only a little compressive stress. Consequently, the decrease in the effective coordination for Tl in $TlNiO_3$ is not so large as for Dy in $DyNiO_3$. The large unit cell volume may also be attributed to the different effective coordination number of Tl.

Magnetic susceptibility and local structure around Ni(III)

The molar magnetic susceptibility, χ_m of $TlNiO_3$ shows a maximum at 105 K (Fig. 6). The increase below 30 K might be either due to the presence of a small amount of paramagnetic impurity or due to the surface contribution of fine particles. The thermal variation of the reciprocal molar magnetic susceptibility shows a slight deviation from Curie–Weiss paramagnetic behavior above the Néel temperature.

The slope of χ_m^{-1} *versus* T increases in the temperature range from T_N to about 200 K, and then slightly decreases in the high temperature range (>250 K). This complex behavior is probably rationalized by two effects—short range interaction and temperature independent paramagnetism (χ_{TIP}). According to the effective field approximation, one should take into account the fact that the neighboring spins are correlated with each other due to the formation of magnetic clusters beyond the ordering temperature. The simple treatment proposed by Oguchi allows the expression of the paramagnetic susceptibility beyond the transition temperature as follows:[21]

$$\chi = \frac{C}{T}\frac{4}{e^{-2j}+3-2(z-1)j} \qquad j = \frac{J}{k_B T}$$

where J is the exchange energy and z is the number of nearest neighbors. For a very high temperature, $J \ll 1$, and $e^{-2j} = 1-2j$, which gives the result of the Weiss mean-field approximation:

$$\chi = \frac{C}{T - \frac{1}{2}z\frac{J}{k_B}} = \frac{C}{T-\theta}$$

where θ is the Weiss molecular field Curie temperature. However, as T approaches the ordering temperature, an effective field originating from short-range order becomes important and, consequently, the χ_m^{-1}/T plot shows positive curvature. The experimental data for $TlNiO_3$ were fitted to the function, $\chi_{exp} = \chi + \chi_{TIP}$, where the temperature independent term, χ_{TIP}, includes ion core diamagnetism, Van Vleck paramagnetism and Pauli paramagnetism. This fit gives the value of $C = 0.358$ emu K mol^{-1}, $z = 3.2$, $J/k_B = -76.3$ K^{-1} and $\chi_{TIP} = 420 \times 10^{-6}$ emu mol^{-1}. The effective magnetic moment, μ_{eff}, is determined as 1.69 μ_B, which is comparable to the theoretical *spin only* value of 1.73 μ_B expected for $S = 1/2$. The χ_{TIP} value found is in-between those for $NdNiO_3$ (970×10^{-6} emu mol^{-1})[22] and $La_2Li_{0.5}Ni_{0.5}O_4$ (50×10^{-6} emu mol^{-1}).[23] The θ value is estimated to be -122 K from the values of z and J/k_B. This fitting result supports the view that there is a strong contribution from short range interactions to the magnetism of $TlNiO_3$.

Another important magnetic aspect of $TlNiO_3$ is that the Neel temperature ($T_N = 105$ K) is much lower than those in other rare earth nickel(III) perovskites, such as $YNiO_3$ ($T_N = 145$ K) and $LuNiO_3$ ($T_N = 130$ K). The evolution of T_N's for various $ANiO_3$ (A = rare earth or yttrium) has been explained by means of the Ni–O–Ni superexchange angle.[9] The T_N value decreases monotonically with decreasing the angle for this series of compounds. The average Ni–O–Ni bond angle (147.6°) for $TlNiO_3$ is, however, comparable to that of $YNiO_3$ (147.3°) and it is much larger than that of $LuNiO_3$ (144.6°). The low T_N for $TlNiO_3$, in spite of the large superexchange angles, might originate from the different acidity of Tl(III) and rare earth ions. It has been suggested that the greater the acidity of the A cation, the more strongly it competes for the electron density on the oxygen ions and, hence, the less charge density is available to promote interactions between the magnetic B ions in the ABO_3 perovskite structure.[24] Due to the strong acidity of the Tl(III) ion, an orbital overlap between Ni(III) ions and oxygen ions would be quite weak in $TlNiO_3$, leading to a decrease of superexchange energy.

Conclusions

$TlNiO_3$ perovskite has been prepared from the precursors Tl_2O_3, $Ni(OH)_2$ and $KClO_3$ by using a high pressure technique ($P \geqslant 7.5$ GPa, $650 \leqslant T \leqslant 700$ °C). The larger unit cell volume of $TlNiO_3$ compared to that expected from the *V vs. r* plot for other $ANiO_3$ (A = rare earth or yttrium) materials is due to the different coordination environment around the Tl(III) ion. The strongly covalent Tl–O bonds weaken the Ni–O bonds, leading to a relatively weak orbital overlap between Ni(III) and the oxygen ions. This effect results in a low T_N for $TlNiO_3$ ($T_N = 105$ K) although the superexchange angle Ni–O–Ni (147.6°) is similar to that observed in $YNiO_3$ (Ni–O–Ni bond angle = 147.3°, $T_N = 145$ K). In addition, the deviation of the thermal evolution of the inverse magnetic susceptibility from the Curie–Weiss law above T_N is rationalized by the short-range interaction.

Acknowledgements

We would like to thank Professor Jean Etourneau, for fruitful discussions. We also thank the French Ministry of Foreign Affairs for supporting S.-J. K., the recipient of a Pasteur scholarship. This work was in part supported by the Korean Ministry of Education through the Korea Research Foundation (1997-011-D0019) and the BK21 program, and also by the Korean Ministry of Science and Technology through the NRL project.

References

1 G. Demazeau, A. Marbeuf, M. Pouchard and P. Hagenmuller, *J. Solid State Chem.*, 1971, **3**, 582.
2 G. Demazeau, A. Marbeuf, M. Pouchard, P. Hagenmuller and J. B. Goodenough, *C. R. Seances Acad. Sci., Ser. C*, 1971, **272**, 2163.
3 G. Demazeau, *Thèse ès Sciences doctorat*, University of Bordeaux, 1973.
4 J. B. Torrance, P. Lacorre, A. I. Nazzal, E. J. Ansaldo and Ch. Niedermayer, *Phys. Rev. Sect. B*, 1992, **45**, 8209.
5 M. Medarde, *J. Phys.: Condens. Matter.*, 1997, **9**, 1679.

6 J. Rodriguez-Carvajal, S. Rosenkranz, M. Medarde, P. Lacorre, M. T. Ferández-Diaz, F. Fauth and V. Tronnov, *Phys. Rev. Sect. B*, 1998, **57**, 456.
7 M. Medarde, P. Lacorre, K. Conder, F. Fauth and A. Furrer, *Phys. Rev. Lett.*, 1998, **80**, 2397.
8 J. A. Alonso, M. J. Martínez-Lope, M. T. Casais, M. A. G. Argenda and M. T. Ferández-Diaz, *J. Am. Chem. Soc.*, 1999, **121**, 4754.
9 J. A. Alonso, J. L. García-Munoz, M. T. Ferández-Diaz, M. A. G. Argenda, M. J. Martínez-Lope and M. T. Casais, *Phys. Rev. Lett.*, 1999, **82**, 3871.
10 J. A. Alonso, M. J. Martínez-Lope, M. T. Casais, J. L. García-Munoz and M. T. Ferández-Diaz, *Phys. Rev. Sect. B*, 2000, **61**, 1756.
11 P. M. Woodward, *Acta Crystallogr., Sect. B*, 1997, **53**, 44.
12 R. D. Shannon, *Inorg. Chem.*, 1967, **6**, 1474.
13 J. Bassett, R. C. Denney, G. H. Jeffery and J. Mendham, *Vogel's textbook of quantitative inorganic analysis*, 4th edn., Longman Inc., New York, 1978.
14 J. Rodriguez-Carvajal, FULLPROF, ver. 3.2, LLB-CEA, Saclay, France, 1997.
15 *International Tables for Crystallography*, Kluwer Academic, Dordreacht/Boston/London, 1989, vol. A.
16 R. D. Shannon, *Acta Crystallogr., Sect. A*, 1976, **32**, 751.
17 M. Marezio, J. P. Remeika and P. D. Dernier, *Acta Crystallogr., Sect. B*, 1970, **26**, 2008.
18 S. Quezel-Ambunaz and J. Mareschal, *Bull. Soc. Fr. Mineral. Cristallogr.*, 1963, **86**, 204.
19 E. J. Little and M. M. Jones, *J. Chem. Educ.*, 1960, **37**, 231.
20 N. E. Brese and M. O'Keeffe, *Acta Crystallogr., Sect. B*, 1991, **B47**, 192.
21 J. S. Smart, *Effective field theories of magnetism*, W. B. Saunders, Philadelphia and London, 1966.
22 J. Blasco, M. Castro and J. García, *J. Phys.: Condens. Matter*, 1994, **6**, 5875.
23 Z. L. Ming, G. Demazeau, M. Pouchard, J. P. Dance and P. Hagenmuller, *J. Solid State Chem.*, 1989, **78**, 46.
24 J. B. Goodenough, *Magnetism and the chemical bond*, Interscience, New York, 1963.